Ibn Al-Haitham Journal for Pure and Applied Sciences
Journal homepage: jih.uobaghdad.edu.iq
PISSN: 1609-4042, EISSN: 2521-3407
IHJPAS. 2025, 38(4)

A New Green CFIA/MZT System for Spectrophotometric Determination of Anthranilic Acid

Jehan Sh. Hussien[1*] and Bushra B. Qassim[2]
[1,2] Department of Chemistry, College of Sciences, University of Baghdad, Baghdad, Iraq.
*Corresponding Author.

Received:24 April 2025 Accepted: 21 July 2025 Published: 20 October 2025
doi.org/10.30526/38.4.4155

Abstract

Anthranilic acid (AA) was determined in pure material via a new system of the CFIA method that involves less chemical consumption (µL), is rapid, semiautomated, simple, and accurate. Two reactions of the AA were conducted; the first, with 4-amino antipyrine and potassium periodate as the oxidizing agent, yielded a pinkish-violet colored product, which was measured at λmax 550 nm. The second reaction, using 2,2`-bipyridine with FeCl3, produced a Pinkish-red product, which was measured at λmax 521 nm. Other chemical and physical factors that affect the stability of the complex products in the suggested process include flow rate, reagent concentration, sample volume, dispersion, and reaction coil. The linearity ranges were (10-400) and (5-150) µg.mL^{-1}, the average recovery percentages were 100.995 and 100.974, while the error percentages were 0.995 and 0.974, respectively. The detection limit values were 1.63 and 0.69 µg.mL^{-1}, respectively. A relative standard deviation of 0.28% and 0.65% was observed, and the sample throughput was 80 and 90 samples/hour, respectively. The devised approach was tested against the conventional method and was shown to be more sensitive. Moreover, a t-test was used to contrast "true value" with "practical value". At the 95% confidence level, it was found that the values were not significantly different.

Keywords: Anthranilic acid, 4-Amino antipyrine, 2,2`-Bipyridine, Continuous flow-injection analysis merging zones technique, Potassium periodate.

1. Introduction

Anthranilic acid (AA), synonymous with *O*-aminobenzoic acid, formula $C_6H_4(NH_2)(COOH)$, the M.wt was 137.14 g mol^{-1}, D was 1.412 g cm^{-3}, and (m.p.) was 146-148^0 C and a b.p. of 200ºC (1). The compound is classified as aromatic due to its two neighboring functional groups: a carboxylic acid and an amine. This classification is further supported by the 'ortho' (a replaced benzene ring) structure, which renders the substance amphoteric. The AA derivatives are regarded as an inexpensive and effective starting point for the synthesis and manufacturing of several commercially available medications. A variety of AA analogues have been shown to have biological activity as well as possible anticancer, antibacterial, insecticidal, antiviral, and anti-inflammatory properties (2-4). An essential component of almost 70 medicines, 50 clinical medications, 20 agrochemicals, and a variety of fine chemicals is AA. Every year, more than 400,000 tons are generated for the

manufacturing of agrochemicals (5). Industrially, AA is an intermediate in the production of azo dyes and saccharin. Besides, AA and its analogues form a functional pharmacophore in the Glafenine, Floctafenine, and Fenamates. They are classified as anti-inflammatory drugs and antibiotics, and serve as the basis for the synthesis of medicinal products like Methaqualone, which is available under the trade name Mandrax (6). Several analytical methods for the determination of AA in various forms, including the spectrophotometric method (7), potentiometric titration (8), fluorometric (9), liquid chromatography (10), and high-performance liquid chromatography (HPLC) (11), are delicate. Still, they all require expensive and time-consuming equipment. Conversely, continuous flow-injection analysis merging zones (CFIA/MZ) is a green analytical method and environmentally friendly because it offers several advantages in analytical chemistry, including being economical, having reduced chemical consumption, being semiautomatic, and enabling high sampling (12-16). Many studies have worked in this field using a different FIA system (17-21) that has one channel manifolds/MZT. This study aims to determine of AA in pure material via the developed green CFIA systems through a new oxidative coupling reaction with a suitable coupling agent.

2. Materials and Methods

A Shimadzu UV-1800 UV-VIS A spectrometer (Japan) was employed for determining all of the absorption in the batch process. A modified detection device has an F.C. composed of quartz silica (1 cm) with a volume of 80 µL. **Scheme 1** shows the suggested FIA/MZT in this technique.

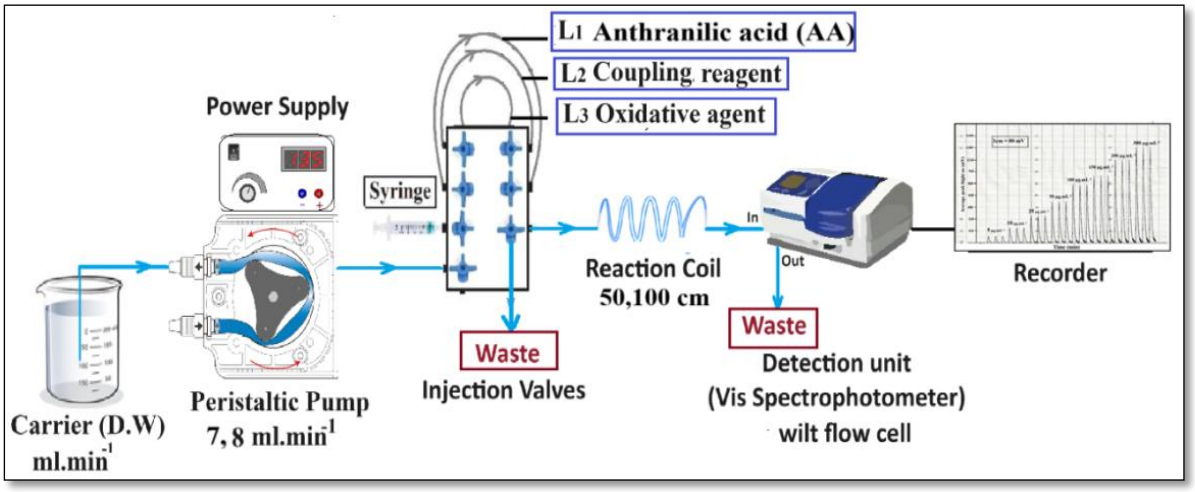

Scheme 1. The manifold module of the developed CFIA/MZ system for determination of AA.

A single-channel system that was developed using distilled water (D.W.) as a carrier at a rate of mL/min through the seven-three-way injection valve. A peristaltic pump (Master Flex C/L, USA) was used to squeeze the D.W., which travels at 90°, containing (3) loops made of Teflon (I.D. 0.5 mm), and was used for loading the organic acid AA or its derivative in L1, the coupling reagent in L2, and the oxidizing agent in L3. The substances are mixed using a glass R.C. (2 mm, I.D.). Each measurement and absorbance spectrum made during the developed FIA investigation was performed by the improved Optima photometer (301, the defendant), a single-beam VIS-Spectrophotometer, Japan. The absorbance can be measured with the Kompensograph C1032 (Siemens) or an optical multimeter (DT9205A, OVA, China). It was calculated as the average peak height of responses (n=3) in mV. The analytical class contributed all of the experimental materials, reagents, and solvents used in this

research, and all concentrations previously generated.

Standard AA 98% (M.wt= 137 g.mol^{-1} BDH): 1000 µg. mL^{-1}. A stock solution of AA was prepared by weighing 0.0500 g of pure substance, dissolving it in 5 mL of methanol, and completing the volume to 50 mL in a volumetric flask with D.W.

Reagent's stock; 4-amino antipyrine (4-AAP ≥ 97%) M.wt= 203 g.mol^{-1}, Merck Germany 1×10^{-3} M, 0.0203 g of the reagent was dissolved in 100 mL volumetric flask with D.W, and 3×10^{-3} M of 2,2-bipyridine (BPY 98%, M.wt=156.19 g.mol^{-1}, BDH) dissolved 0.0468 g in 5mL of ethanol, then completed with D.W. in a 100 mL volumetric flask.

Oxidizing agent's stock solution; Potassium periodate (KIO_4 99.8%) M.wt 230 g.mol^{-1}, Merck Germany 1×10^{-4} M, was preparing by dissolved 0.0023 g in 100 mL vol. flask with D.W., $FeCl_3$ 37.5%) (M.wt= 162.2 g.mol^{-1}, Merck) 1×10^{-4} M. A 0.0016 g of $FeCl_3$ was dissolved in 0.5 mL of HCl 35%, w/w, 1.19 g.mL^{-1}, BDH, 0.1 mol.L^{-1} and completed to100 mL with D.W.

Interference preparation: 0.05 g of each of the interfering substances (sucrose 99.9%, cellulose 99.8%, lactose 99%, glucose 99.9% and sodium citrate 99%) was dissolved in 50 mL of D.W.

3. Results

3.1. Suggested reactions of anthranilic acid with 4-amino antipyrine and bipyridine

Determination of 25 µg.mL^{-1} AA based on coupling with 3×10^{-3} M of 4-AAP in 5×10^{-4} M of KIO_4 as oxidizing agents in a 10 mL volumetric flask to create a colored complex (pink-violet) using a spectrophotometric approach, measured at λ_{max} 550 nm, as shown in **Figure 1** and **Scheme 2**.

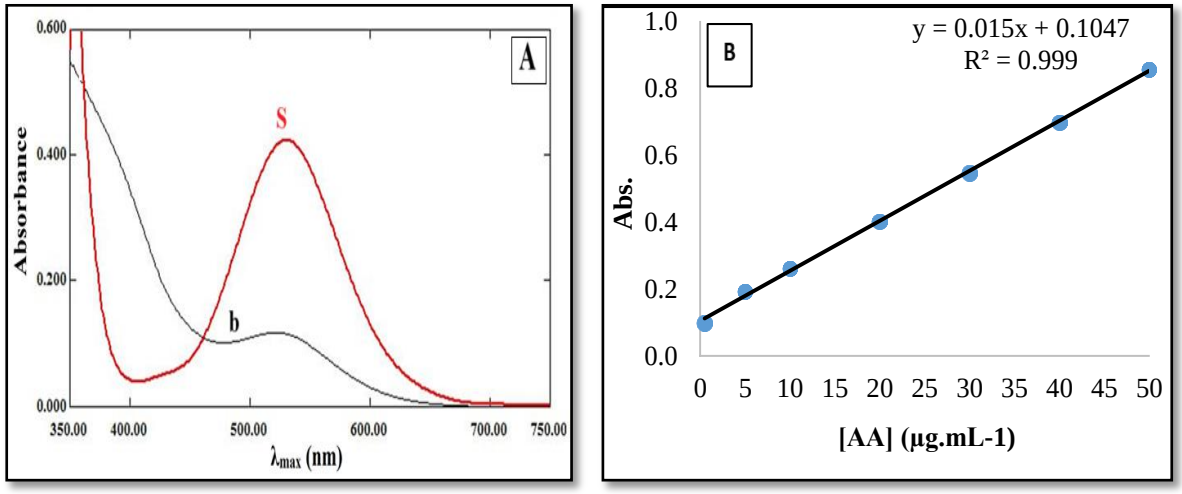

Figure 1. A- Absorption spectrum of 25 µg.mL^{-1}AA**;** (S) Pink-violet colored product against blank solution. b. Blank solution (4-AAP+KIO_4). **B-** Linear calibration curve estimation for AA organic acid using the classical method.

Spectrophotometric determination of 25 µg. mL^{-1} AA based on coupling with 2×10^{-3} M BPY in the presence of 3×10^{-4} M of $FeCl_3$ as oxidizing reagent in a 10 mL volumetric flask to yield (pink-red) compound was scanned at λ_{max} 521 nm as shown in **Figure 2** and **Scheme 3**.

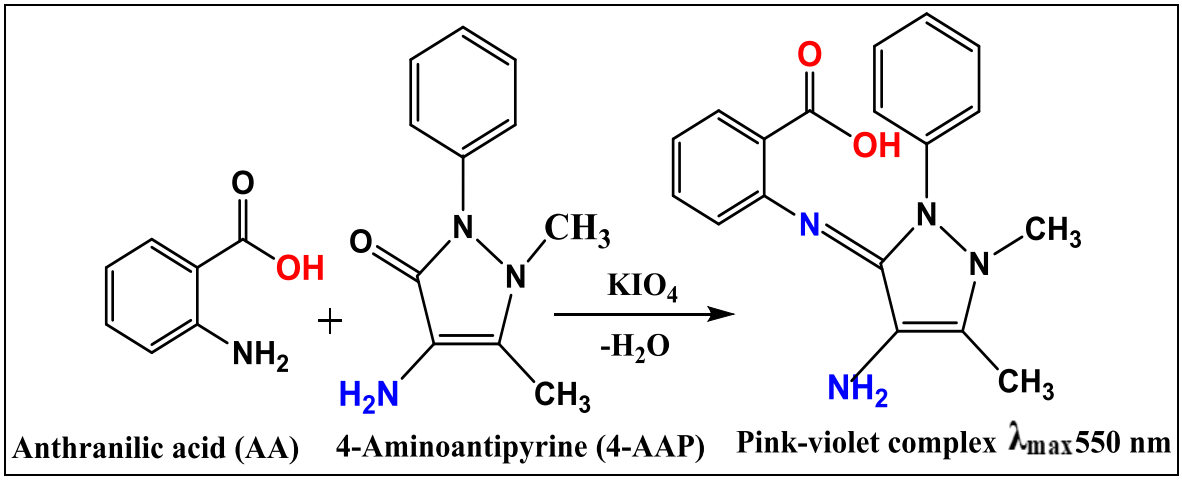

Scheme 2. Proposed reaction of AA and 4-AAP.

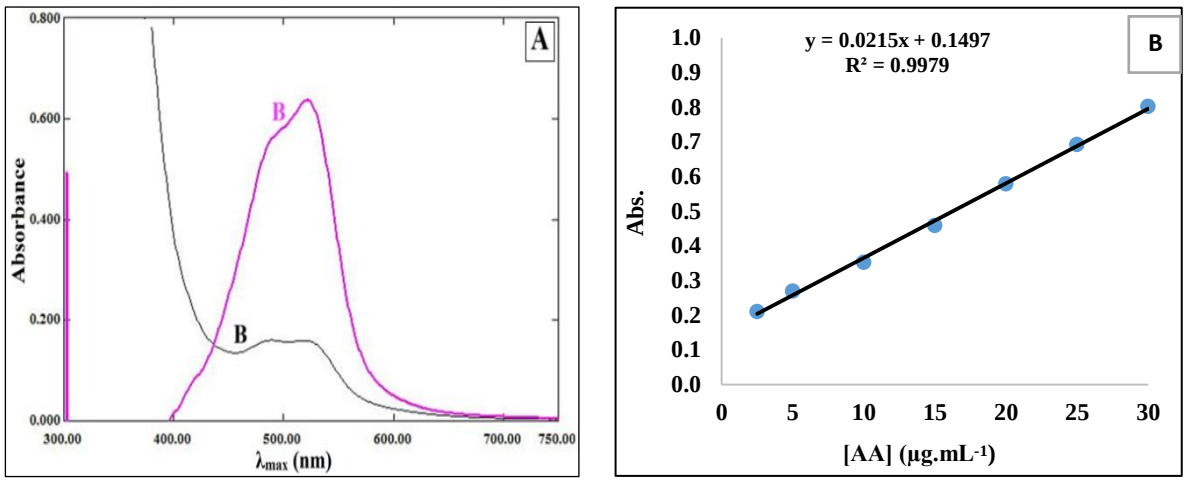

Figure 2. The Absorption spectrum of 25 µg. mL^{-1} AA; **A-** Pink-red colored product against blank solution BYP, $FeCl_3$. **B-** Linear calibration curve for the determination of AA using the classical method.

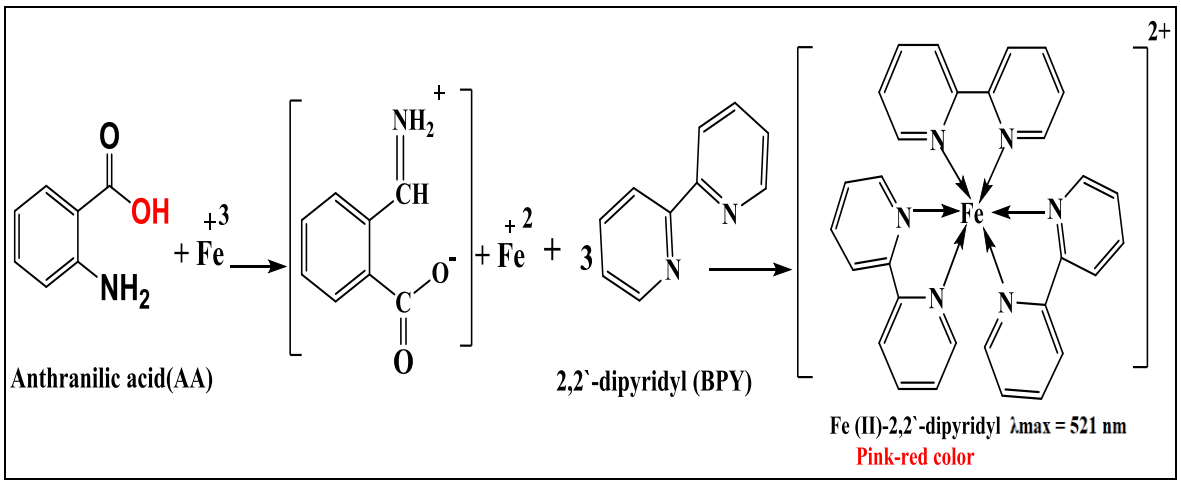

Scheme 3. Propose a mechanism of the reaction for AA with BPY using the batch method.

3.2. The manifold of the suggested CFIA/MZ system

Chemical optimal conditions were examined for the organic acids (AA). A first experiment was determining the optimal concentration of the reagent (4-AAP), it's found 3×10^{-3} M while for the second reagent BPY optimal concentration was 4×10^{-3} M, as seen in **Figures 3** (A, B), other investigate was ideal concentration of the oxidative agents, KIO_4, $FeCl_3$ were 5×10^{-4} M, 2×10^{-4} M consequently, as seen in **Figure 4 A** and **B**. The better order added was examined, which was (O.A in L1, Ox in L2, and R in L3) for the 1st system and (O.A in L1, R in L2, and Ox in L3) for the 2nd system, as shown in **Figures 5A** and **B**.

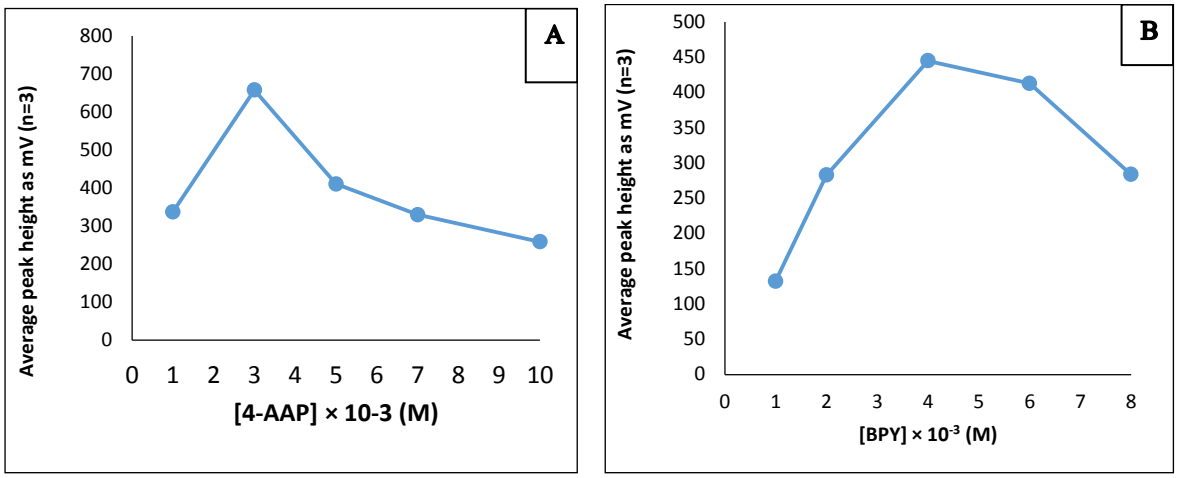

Figure 3. Influence the concentration of reagents **A-** (AA, 4-AAP), **B-** (AA, BPY) in the FIA/MZ system.

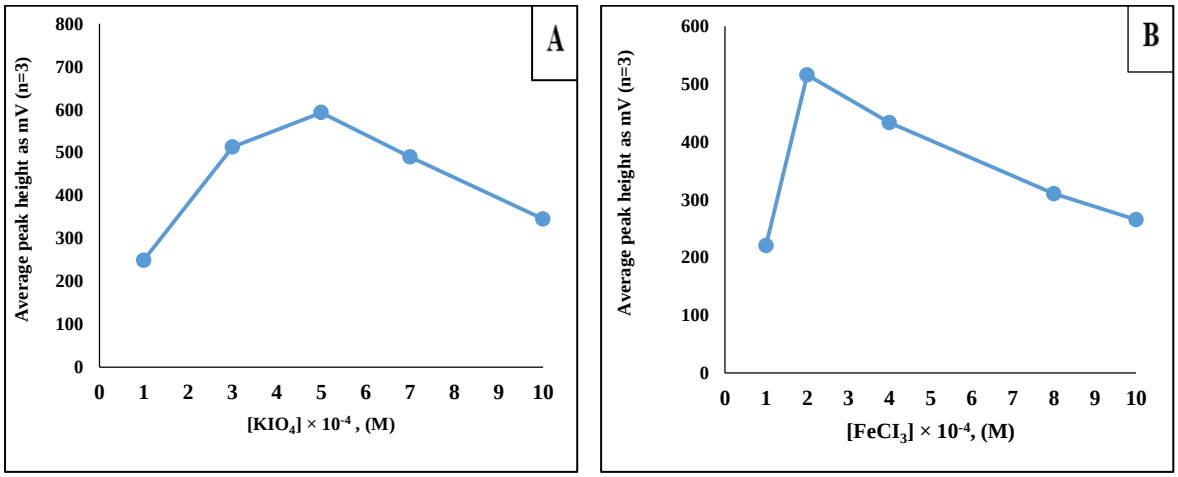

Figure 4. Best concentration of oxidizing agent for two CFIA systems. **A-** AA with KIO_4. **B-** AA with $FeCl_3$

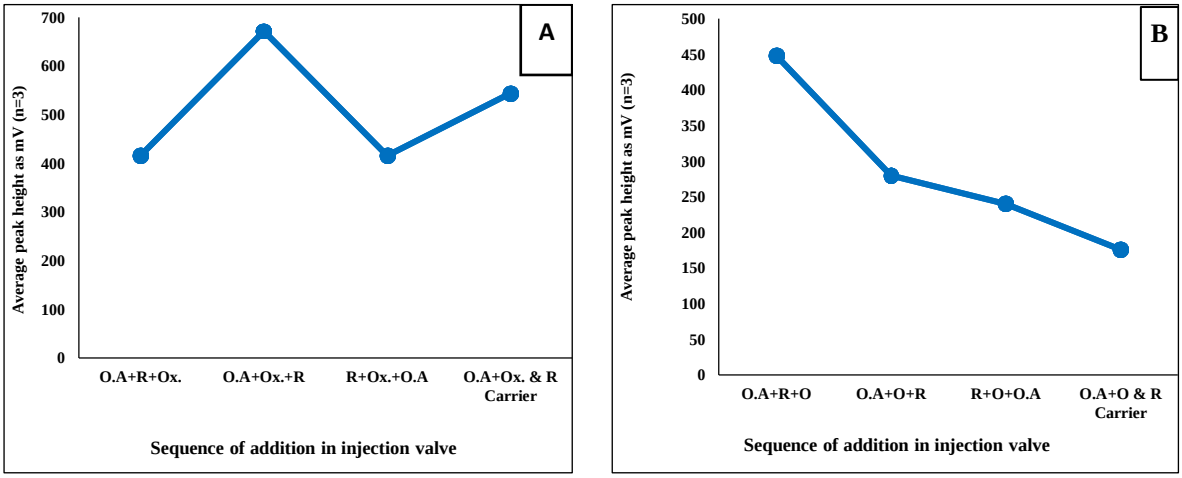

Figure 5. Sequence of chemicals addition which loaded in L1, L2, L3. **A-** (AA+4-AAP), **B-** (AA+BPY).

3.3. Physical variables

A flow rate was studied for both reactions, so the optimum flow rate was found to be 7-8 mL/min, as shown in **Figure 6 A, B**. While the optimum length of the R.C. of new CFIA systems was (100,50) cm consequently for the two reactions, as shown in **Figure 7 A** and **B**.

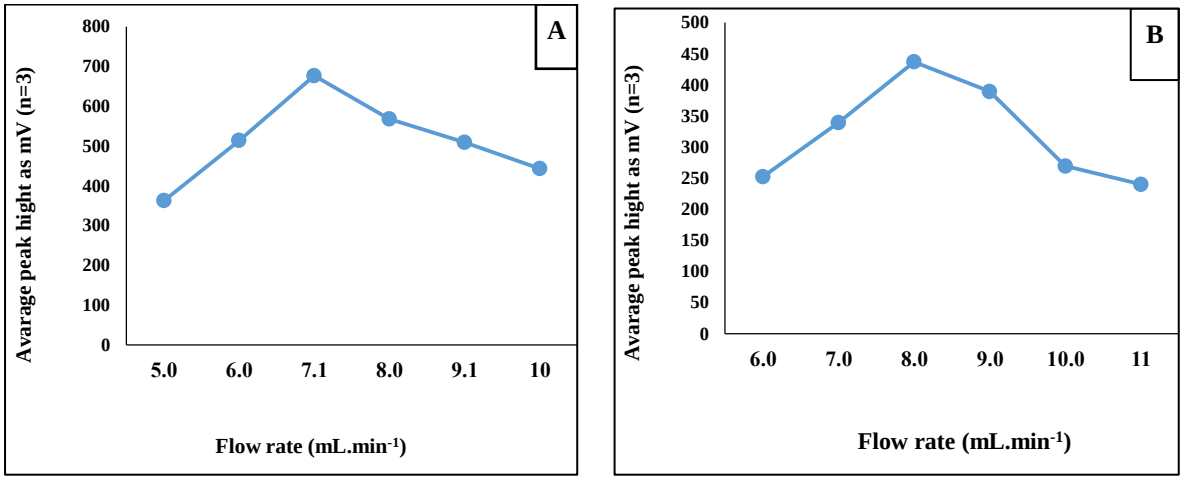

Figure 6. Influence of flow rate **A-** AA with 4-AAP, **B-** AA with BPY.

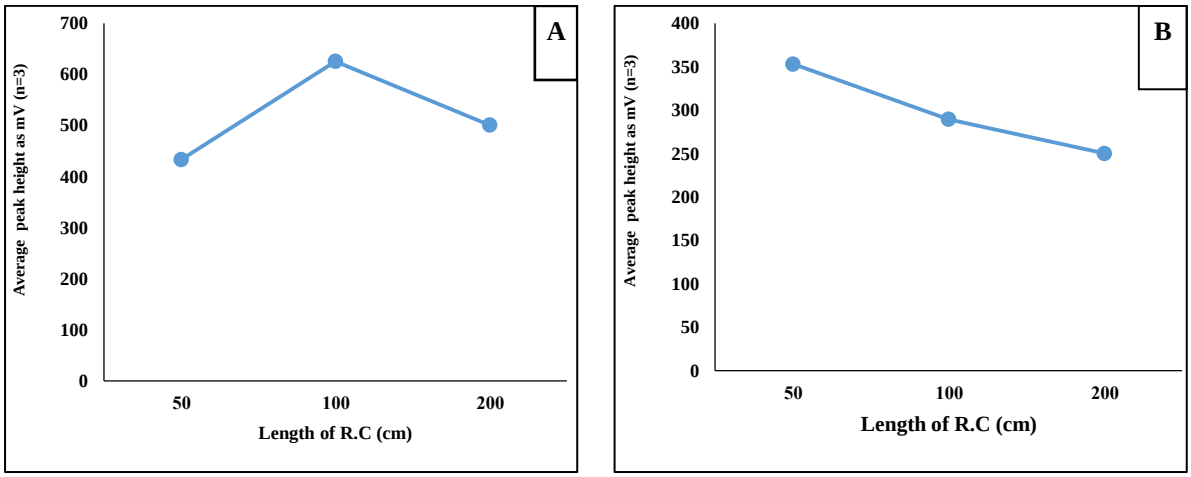

Figure 7. Effect of reaction coil of **A-** AA (4-AAP), **B-** AA (BPY) of CFIA systems.

Therefore, the sample throughput is about 80,90 samples/hour, for the first and second reaction, respectively, which is calculated by finding the time required to inject the solutions into the seven three-way injection valve loops. It took nearly 15 seconds to find the time needed to reach the maximum peak height. It was nearly 30.25 seconds. The optimal size loops for the AA tow reaction were 40-40-40 cm; (78.50-78.50-78.50) µL and 30-30-40 cm; (58.88-58.88-78.50) µL, as shown in **Figure 8 A** and **B**.

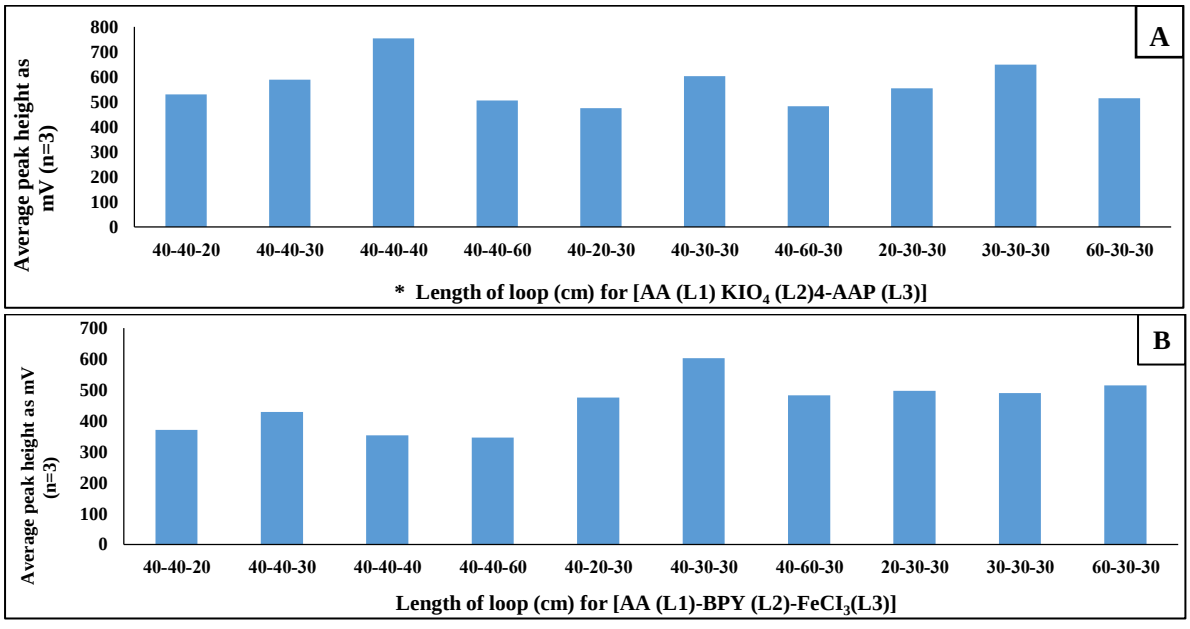

Figure 8. Effect of injected volume in CFIA systems AA **A-** with 4-AAP. **B-** with BPY.

3.4. Dispersion

The estimated dispersion of AA is calculated using the equation, mD= Co/C, as shown in **Table 1**.

Table 1. Dispersion value of the two reactions of [AA- 4-AAP], [AA-BPY] via flow injection.

[AA-4-AAP] µg.mL^{-1}	*C_o(cm)	*C_{max}(cm)	*D	[AA+BPY] µg.mL^{-1}	*C_o(cm)	*C_{max}(cm)	*D
50	5.8	0.083	1.261	25	4.0	3.3	1.212
200	10.8	0.1	1.286	75	8.0	6.2	1.290

*D; Dispersion, C_o; The peak without dilution, C; The peak after dilution.

3.5. Calibration curve

Preparation of a sequence of AA solutions from 1-1000 µg.mL^{-1}, followed by injection into the developed unit with reagent 4-AAP and the oxidative agent KIO_4 (10-400 µg). mL^{-1}, the linear range of AA, as shown in **Table 2** and **Figure 9 A** and **B**.

Preparation of a sequence of AA solutions from 1-1000 µg.mL^{-1}, then injection on the developed unit with the reagent BPY and the oxidative agent $FeCl_3$, the linear range of AA (5-150) µg.mL^{-1}, as shown in **Figure 10** and **Table 3**.

Table 2. Linear calibration curve for determination of AA with 4-AAP via FIAT using KIO_4.

[AA-4AAP] (µg.mL^{-1})	Average response ($\bar{y}$) (mV)	RSD%	S.E.M	*E/y %
10	228	0.26	227.93±1.48	0.65
25	289	0.28	289.43 ±2	0.69
50	349	0.13	348.99 ±1.13	0.32
100	483	0.19	483.17 ±2.26	0.47
200	680	0.03	680.26 ±0.47	0.07
300	925	0.10	925.33±2.29	0.25
400	1121	0.52	1121 ±14.41	1.29

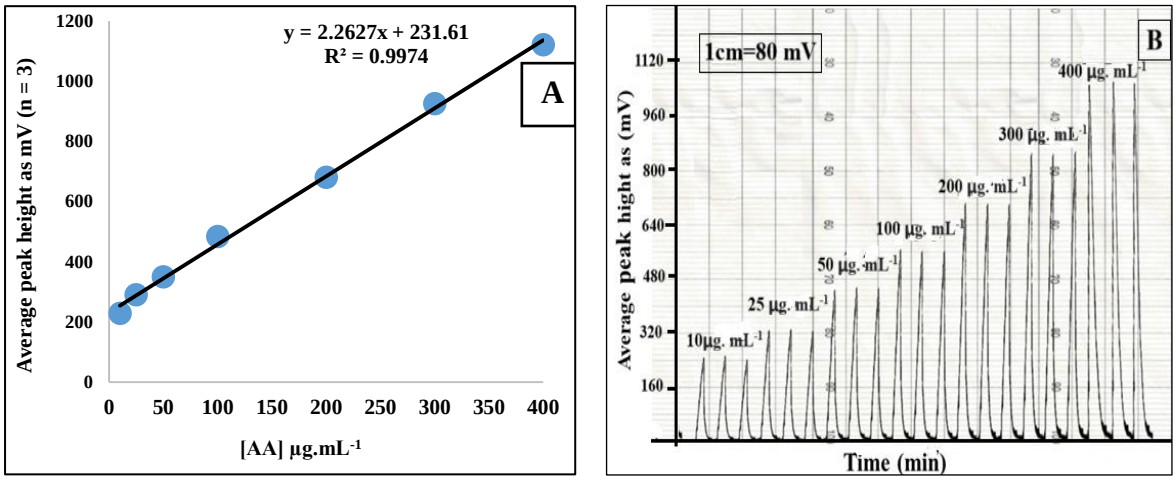

Figure 9. **A-** Linear calibration curve for detection of AA, 4-AAP via the suggested CFIAT. **B-** Response variation with increasing of concentrations of (AA,4-AAP) via the developing CFIAT.

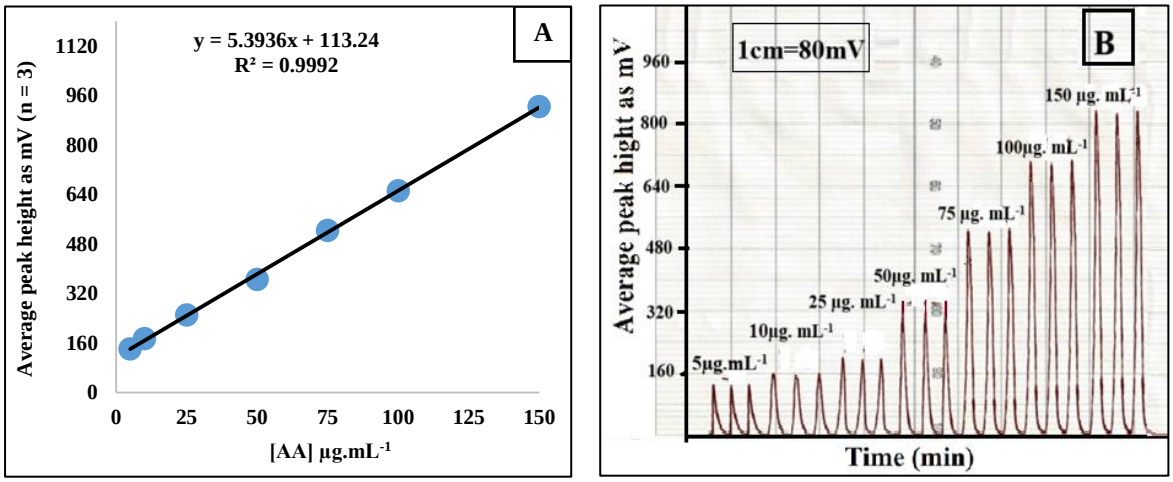

Figure 10. A- Linear calibration curve for determination of AA via the suggested CFIAT.B- Response variation with increasing of concentrations of (AA, BPY) via the CFIA.

Table 3. Linear calibration curve for evaluations of AA-BPY in FIAT using $FeCl_3$.

[AA-BPY] (µg.mL^{-1})	Average response ($\bar{y}$) (mV)	RSD%	S.E.M	*E/y %
5	141	0.40	140.78±1.41	1.00
10	173	0.45	289.43 ±1.94	1.12
25	267	0.61	348.99 ±4.01	1.50
50	380	0.22	483.17 ±2.07	0.54
75	502	0.12	680 ±1.52	0.30
100	651	0.27	500.89±1.52	0.25
150	909	0.09	909.45 ±1.95	0.21

*Average peak height (n=3) expressed as mV, *ŷ= bx+ a at different concentration (x), *S.E.M= $\bar{y} \pm t_{0.05}$ ($\boldsymbol{\sigma_n - 1\sqrt{n}}$) *$E/y\% = t_{tab}\, SD/\sqrt{n} \times 100\ \%/\ \bar{y}$.

The repeatability was calculated for the first and second reactions by choosing two different concentrations of AA (50,200) µg and (25,75) µg.mL^{-1}; consequently, it is included in the calibration curve using the developed CFIAT(n=8) as shown in **Tables 4** and **5**.

Table 4. Repeatability of successive measurement of AA-4-AA, (n=8) using the FIA system.

[AA-4-AAP]	Found	Error	Rec%	Erel%	RSD%
50	51.293	1.293	102.586	2.586	0.398
200	197.827	2.173	98.913	-1.087	0.272

Table 5. Repeatability of successive measurement of AA-BPY, (n=8) using FIA system.

[AA-BPY]	Found	Error	Rec%	Erel%	RSD%
25	25.406	0.406	101.626	1.626	0.550
75	75.242	0.242	100.322	0.322	0.744

3.6. Analysis of variance

Determination of the sum of squares (SS) of the variance values (ŷi) based on the regression's average value. The value (F) is obtained by dividing the result by the square root of the degrees of freedom (1), as shown in **Tables 6** and **7**.

Table 6. Analysis of variance for the suggested CFIA system for AA-4-AAP.

Source of Variation	SS	Df	MS	*Fcal.	F crit
*Between Groups (error)	1237303.1428	1	1237303.1428	21.4124	4.7472
*Within Groups (regression)	693412.57142	12	7784.380952		
Total	193071557	13			

Table 7. Analysis of variance for the suggested CFIA system for AA-BPY.

Source of Variation	SS	Df	MS	*F cal.	F crit
*Between groups (error)	656211.50	1	656211.50	16.1153	4.7472
*Within groups (regression)	488636.00	12	40719.67		
Total	11448475	13			

*Between groups (error) =$\sum$ni ($\bar{y}$i- $\bar{y}_{GM}$)^2. *Within groups (regression)=$\sum$(ni-1) S_1^2, *F cal=F$(S_1)^2$/ F$(S_2)^2$.

3.7. Analytical characteristic of the developed methods

Calibration curve as S.E.M for determination of AA with (4-AAP,BPY) using a new CFIA/MZT is shown in **Table 8**.

Table 8. Calibration curve as S.E.M for determination of AA with (4-AAP, BPY) using a new CFIA/MZT.

Parameters	[AA-4-AAP-KIO_4]	[AA-BPY-$FeCl_3$]
λmax (nm)	550	521
Regression equation; y =bx+ a	y = 2.2627x +231.61	y = 5.3936 x +113.24
Linear range (μg mL^{-1})	10- 400	5-150
$\text{Rec\%} = \frac{\text{Found } (\bar{X})}{\text{Present } \mu} \times 100\%,$	100.995	100.974
$\text{Erel\%} = \frac{\text{Found } (\bar{X}) - \text{Present } (\mu)}{\text{Present } (\mu)} \times 100\%$	0.995	0.974
$\text{RSD\%} = \frac{\text{Standard Deviation of five determinations}}{\text{The Average of the determinations}} \times 100\%$	0.280	0.647
Intercept (a); (a = y– b x)	231.61	113.2409
Slope (b); (mL. μg^{-1}) b = Σi [(xi –$\bar{x}$) (yi – $\bar{y}$)]/Σi(xi –$\bar{x}$)^2)^2	2.2627	5.3936
Linearity (R^2%)	0.9974	0.9992
(r): r=Σi [(xi –$\bar{x}$) (yi – $\bar{y}$)] [(Σi (xi –$\bar{x}$) ^{2}) (Σi (yi – $\bar{y}$)^2)]$^{0.5}$	0.9987	0.9996
(S_b)Sb = $S_{y/x}$ /[Σi(xi –$\bar{x}$) ^{2}]$^{0.5}$	0.0521	0.0685
(S_a) $\boldsymbol{Sa = Syx\ \sqrt{n\Sigma(xi-\bar{x})\ i^2}}$	10.8375	5.2644
(LOD)	1.6341	0.6855
(LOQ)	5.4469	2.2850
Through put (Sample .h^{-1})	80	90
$S_{y/x}$ = [Σi (yi – ŷi)^2 / (n – 2)]$^{0.5}$; ŷi =bxi+a	19.1356	8.8677
$C_{.l}$ slope (b) = b ± tSb	2231.61±t 0.05	5.3936 ± t 0.0685
$C_{.l}$ intercept (a) = a ± tSa	2.2627±10.837	113.24 ± t 5.2644

3.8. Interferences

The interferences can be examined, including glucose, sucrose, lactose, cellulose, and sodium citrate, to evaluate the efficacy of the suggested CFIA/MZT, using 100 and 50 μg.mL^{-1} for the two reactions of AA, respectively, of the pure samples of the organic acid.

No interferences were found when determining the organic acid AA using the CFIA technique, as shown in **Table 9**.

The interference effect on the reaction of organic acids via the developed FI system is demonstrated in **Table 10**.

Table 9. Interference effect on the reaction of organic acids via the developed FI system.

	[AA-4-AAP-KIO_4]				[AA-BPY-$FeCl_3$]			
Interference type	**Conc. of interferences ($\mu g.mL^{-1}$)**	**Average response ($\bar{y}$) (mV)**	***Erel %**	***Rec %**	**Conc. of Interferences ($\mu g.mL^{-1}$)**	**Average response ($\bar{y}$) (mV)**	***Erel %**	***Rec %**
Standard	----	300	0.98	100.98	----	361	0.38	100.38
Sucrose	50	298	1.22	101.48	25	542	0.12	100.12
	100	300	-0.52	99.48	50	539	-1.42	98.58
	200	301	0.98	100.98	100	536	0.05	100.05
Lactose	50	461	1.29	101.29	25	531	0.63	100.63
	100	457	-0.24	99.76	50	533	-0.05	99.95
	200	456	-0.78	99.22	100	536	-1.14	98.86
Glucose	50	456	-0.66	99.22	25	362	1.54	101.54
	100	460	-0.95	100.95	50	361	0.78	100.78
	200	456	-0.08	99.92	100	360	-0.44	99.56
Cellulose	50	460	0.98	100.98	25	361	0.88	100.88
	100	456	-0.66	99.34	50	361	0.40	100.40
	200	461	1.22	101.22	100	361	0.69	100.69
Sodium Citrate	50	460	0.98	100.98	25	362	1.43	101.43
	100	458	0.00	100.00	50	359	-1.26	98.74
	200	461	1.22	101.48	100	360	-0.31	99.69

Table 10. Comptonization of the developed CFIA/MZT method for the determination of AA with other methods.

Analytical method	Comment	LOD	Linear range	Ref
Spectrofluorometric	Coupling reaction of the antibiotic with diazotized AA to form a yellow azo dye was shown absorption at 419 nm.	0.2813 $\mu g.mL^{-1}$	0.5-60 $\mu g.mL^{-1}$	27
Potentiometric titration	The acid-base equilibrium of AA have been characterized micro dissociation constants	-------	--------	28
Electrochemical sensor	Determine of AA has emerged as a possible moderator for use in co-polymer systems.	2.13 nM	1.0×10^{-8} - 4.0×10^{-4} M.	29
HPLC	The separation was performed on a C18 column using the mobile phase-buffer (potassium dihydrogen ortho)	10 -50 µg/mL	0.99 $\mu g.mL^{-1}$	30
Voltammetry	Voltametric techniques in pH 5.0 phosphate buffer solutions with ionic strength 0.2M.	1.94 nM	1.0×10^{-8}- 3.0×10^{-6} M	31

4. Discussion

The dispersion value in this study was 1.2 for both reactions. A carrier was D.W. in the FIA/ MZT, which is in agreement with previous studies (22)**.** The analysis of variance test is a way to discover if significant findings are obtained, which aid in determining the calibration curve required to accept the alternative hypothesis or reject the null hypothesis. To estimate $(yi-\hat{y}i)^2$ for (n-2), compute the sum of squares of the difference between the appraiser's yi values (S2) or the response's (yi) values, the anticipated error, and the called-for regression. The analytical characteristics of both methods (batch and FIA/ MZT) for determination of AA by two reactions [AA-4-AAP-KIO_4] and [AA-BPY-$FeCl_3$] such as (Rec%), (Erel%), (LOD) (20), (LOQ), (Ɛ), Sandals sensitivity (S), ($S_{y/x}$), Confidence limit of slope (CL_b) and (CL_a) were calculated (23). The confidence limit was 95% and the degrees of freedom (n-2). It is clear from the current findings, that the methods proposed in the research manuscript are new and have not been previously addressed in the field of flow injection analysis and have many advantages: simple, fast, sensitive, and highly modeled with analysis

per hour without the need for separation or extraction processes and the use of solvents or expensive equipment, especially since AA has great importance as it is used in industry as an intermediate material for the production of azo dyes and saccharin, and in the preparation of perfumes to imitate the scents of jasmine and orange, and in pharmaceutical preparations as a diuretic, which is in agreement with previous data (24-27). The AA spiked with a half, equal, and double increments of interfering concentration. Absolute error and increase in the interference concentration do not affect the response intensity value with high organic acid recoveries (28, 29)

5. Conclusion

The proposed method in this study is classified as green chemistry for the determination of aromatic organic acid (AA), which has a sweetish taste, using a new type of flow injection analysis technology (friendly to the environment) by consuming small amounts of microliter volumes of the organic acid. Toxic organic reagents were used to complete the reactions. Following an examination and evaluation of the scientific literature within the CFIA systems, it was found that there is currently no published work for the determination of the AA in pure material and estimation of its biological activities. So, the unique and novel study concept was to use the CFIA/MZT for the spectrophotometric determination of AA. The advantages of the proposed CFIA method include simplicity, sensitivity, a wide operating range, semi-automated determination of analyte without the need for a pretreatment step or extraction, high recovery, and its highest applications in analytical chemistry.

Acknowledgment

The authors thank their colleagues at the College of Sciences, University of Baghdad, for their cooperation in completing this work, and they appreciate everyone who participated in the study.

Conflict of Interest

The authors declare that they have no conflicts of interest.

Funding

None.

Ethical Clearance

The Scientific Committee at the Department of Chemistry, College of Science, University of Baghdad, has approved this work.

References

1. Ahmed AA, Musa SA, Fugu MB, Mohammed AI, Adam HB, Wakil IM. A comprehensive review on anthranilic acid-derived Schiff bases and their metal chelates: Structures and applications. Chem Rev Lett. 2023; 6(3):350-389. https://doi.org/10.22034/crl.2023.401158.1227.
2. Wiklund P, Bergman J. The chemistry of anthranilic acid. Curr Org Synth. 2006; 3(3):379–402. https://doi.org/10.2174/157017906777934926.
3. Ahmed AA, Aliyu HN. Synthesis, structural characterization and antimicrobial potency of anthranilic acid-based Mn (II) Schiff base complex. Chem Res J. 2019; 4(5):54–61.
4. Nasr TM, Aboshanab AM, Abouzid KA, Zaghary WA. Hands-on synthetic approaches and biological activities of anthranilic acid derivatives: A mini-review. Egypt J Chem. 2023; 66(7): 329–343. https://doi.org/10.21608/ejchem.2022.148409.6426.

5. Li Y, Wang Y, Yang T, Lin Z, Jiang X. Selenium-catalyzed intramolecular atom-and redox-economical transformation of o-nitrotoluenes into anthranilic acids. Green Chem. 2021; 23(8): 2986–2991. https://doi.org/10.1039/D0GC04407E.
6. Prasher P, Sharma M. Medicinal chemistry of anthranilic acid derivatives: A mini review. Drug Dev Res. 2021; 82(7):945–958. https://doi.org/10.1002/ddr.21842.
7. Abou-Zied OK, Al-Busaidi BY, Husband J. Solvent effect on anthranilic acid spectroscopy. J Phys Chem A. 2014; 118(1):103–109. https://doi.org/10.1021/jp410331.
8. Vladescu L, Moja D, Badea I. Determination of anthranilic acid by potentiometric titration. An Univ Bucuresti-Chimie. 2002; 1:97–100.
9. Guidetti P, Walsh JL, Schwarcz R. Fluorometric assay for the determination of anthranilic acid in biological materials. Anal Biochem. 1994; 220(1):181–184 . https://doi.org/10.1006/abio.1994.1310.
10. Schmitt TM, Ziegler RJ, Muzher ES, Doyle RJ, Freers JL. Analysis of anthranilic acid by liquid chromatography. Talanta. 1986; 33(8):657–660. https://doi.org/10.1016/0039-9140(86)80119-7.
11. Anumula KR, Dhume ST. High resolution and high sensitivity methods for oligosaccharide mapping and characterization by normal phase high performance liquid chromatography following derivatization with highly fluorescent anthranilic acid. Glycobiology. 1998; 8(7):6856-6894. https://doi.org/10.1093/ glycob/8.7.685.
12. Hassan B, Hadi H. Development of continuous flow injection analysis method for determination of oxymetazoline and vancomycin hydrochloride in pharmaceutical preparations. Bull Chem Soc Ethiop. 2022; 36(2):303-313. https://doi.org/10.4314/bcse.v36i2.5.
13. Ajam W, Basheer B. A novel approach of CFIA technique for assaying of furosemide (sulfa drug) as antibacterial agent in pharmaceutical and biological samples using potassium ferricyanide as oxidizing agent. IHJPAS. 2023; 36(4):246-261. https://doi.org/10.30526/36.4.3155.
14. Radhia ER, Ali KJ, Hussein FHA. Batch and merging-zone flow injection methods for determination of tetracycline hydrochloride. Curr Chem Lett. 2023;12(4):677–684. https://doi.org/10.5267/j.ccl.2023.6.001.
15. Farhood AS, Taha DN. A new merging-zone flow injection system for the quantification of ferrous and ferric ions in aqueous solution and sludge of wastewater. Anal Sci Technol. 2022;35(5):1–10. https://doi.org/10.5806/AST.2022.35.5.1.
16. Hanooan WA, Qassim BB. A new green approach of CFIA technique for direct assay with a high throughput of sulfamethoxazole drugs using condensation reaction with NQS agent. Baghdad Sci J. 2024; 21(2):0369. https://doi.org/10.21123/bsj.2023.8104.
17. Hamed SL, Qassim BB. A new approach for developing spectrophotometric determination of phenylephrine drug in pure, pharmaceutics and serum samples using sodium periodate as oxidizing agent via a green method of CFIA/merging zone technique. Baghdad Sci J. 2024; 21(1):0081. https://doi.org/ 10.21123/bsj.2023.7671.
18. Farhood AS, Taha DN. A new flow injection system with merging-zone technique for the determination of copper (II) by neocuproine reagent in aqueous solution. Indones J Chem. 2022; 22(1): 770–779. https://doi.org/10.22146/ijc.70799.
19. Muhamad YH, Al-Badri SB. Four injection–single detector merging zone continuous flow injection analysis for determination of ascorbic acid in bell and chili peppers. In: 2nd International Conference on Agriculture, Food Security and Safety. 2021; 2:54–65. https://doi.org/10.32789/agrofood.2021.1005.
20. Chen X, Zhang M, Li X, Xu J, Liang Y. Ammonium determination by merging-zone flow injection analysis and a naphthalene-based fluorescent probe. Talanta. 2023; 256:124274. https://doi.org/10.1016/j.talanta.2023.124274.
21. Kagaya S, Hida-Matsuda K, Tsuzaka S, Minami C, Ide MG, Cattrall RW, Kolev SD. The determination of zinc using flow injection and continuous flow analysis combined with a polymer inclusion film-coated column: Application to the determination of zinc in alloys and commercial lithium chloride. Talanta. 2023; 259:124545. https://doi.org/10.1016/j.talanta.2023.124545.

22. Hamed SL, Qassim BB. Indirect sensitive determination of oxymetazoline. HCl in pure pharmaceutical drugs and biological samples using a modified sensor unit via a green method of FI/MZ system. Chem Rev Lett. 2023; 7(1):95–105.https://doi.org/10.22034/chemm.2023.361846.1607.
23. Hamed SL, Qassim BB. A new approach for developing spectrophotometric determination of phenylephrine drug in pure, pharmaceutics and serum samples using sodium periodate as oxidizing agent via a green method of CFIA/merging zone technique. Baghdad Sci J. 2024; 21(1):0081. https://doi.org/ 10.21123/bsj.2023.7671.
24. Hamed SL, Qassim BB. New green modalities of flow injection technology for assaying anti-allergic drugs in pharmaceutics and biological samples. IHJPAS. 2023; 36(4):288–302. https://orcid.org/0000-0003-4670-7274.
25. Culf AS, Yin H, Monro S, Ghosh A, Barnett DA, Ouellette RJ, Čuperlović-Culf M, McFarland SA. A spectroscopic study of substituted anthranilic acids as sensitive environmental probes for detecting cancer cells. Bioorg Med Chem. 2016; 24(5):929–937. http://dx.doi.org/10.1016/j.bmc.2015.12.044.
26. Vladescu L, Badea I, Moja D. Determination of vitamin H1 by the potentiometric titration. Stud Sci Sci. 2023; 41(1):1–6.
27. McCormick R, Buckley E, Donnelly PJ, Gilpin V, McMath R, Smith RB, Papakonstantinou P, Davis J. Anthranilic acid: a versatile monomer for the design of functional conducting polymer composites. J Compos Sci. 2024; 8(6):208. https://doi.org/10.3390/jcs8060208.
28. Amooshahi P, Khazalpour S, Amani A, Masoumi H. Green electrochemical method for the synthesis of nitro and azo derivatives based on mefenamic acid. Sci Rep. 2022; 12(1):1106. https://doi.org/ 10.1038/s41598-022-05009-0.
29. Malode SJ, Shetti NP, Kulkarni RM. Voltammetric detection and determination of mefenamic acid at silver-doped TiO_2 nanoparticles modified electrode. Mater Today Proc. 2019; 18:671–678. http://dx.doi.org/10.1016/j.matpr.2019.06.464.